THE JOURNAL OF BIOLOGICAL CHEMISTRY
Vol. 275, No. 23, Issue of June 9, pp. 17374–17380, 2000

Printed in U.S.A.

The Orientation of Helix 4 in Apolipoprotein A-I-containing Reconstituted High Density Lipoproteins*

Received for publication, January 5, 2000, and in revised form, March 30, 2000
Published, JBC Papers in Press, April 4, 2000, DOI 10.1074/jbc.M000044200

J. Nicholas Maiorano and W. Sean Davidson‡
From the Department of Pathology and Laboratory Medicine, University of Cincinnati, Cincinnati, Ohio 45267-0529

The three-dimensional structure of the high density lipoprotein (HDL) component apolipoprotein (apo) A-I and the molecular basis for its protection against coronary artery disease are unknown. In terms of discoidal HDL particles, there has been a debate as to the orientation of the apoA-I α-helices around the disc edge. The "picket fence" model states that the α-helical repeats, separated by turns, are arranged parallel to the phospholipid acyl chains of the enclosed lipid bilayer. On the other hand, the "belt" model states that the helical segments run perpendicular to the acyl chains. To distinguish between these models, we used nitroxide spin labels present at various depths in the bilayer of reconstituted HDL (rHDL) to measure the position of Trp residues in single Trp mutants of human proapoA-I. Two mutants were studied; the first contained a Trp at position 108, which was located near the center of helix 4. The second contained a Trp at position 115, two turns along the same helix. The picket fence model predicts that these Trp residues should be at different depths in the bilayer, whereas the belt model predicts that they should be at similar depths. Different sized rHDL particles were produced that contained 2, 3, and >4 molecules of proapoA-I per complex. In each case, parallax analysis indicated that Trp-108 and Trp-115 were present at similar depths of about 6 Å from the center of the bilayer, consistent with helix 4 being oriented perpendicular to the acyl chains (in agreement with the belt model). Similar experiments showed that control transmembrane peptides were oriented parallel to the acyl chains in vesicles, demonstrating that the method was capable of distinguishing between the two models. This study provides one of the first experimental measurements of the location of an apoA-I helix with respect to the bilayer edge.

Although apolipoprotein A-I (apoA-I)[1] was known as a key mediator of high density lipoprotein (HDL) function over 25 years ago (1), little progress has been made in defining the detailed mechanisms underlying its well known protection against coronary artery disease. HDL and apoA-I are thought to be critical for the uptake of cellular cholesterol in the periphery and, after interactions with numerous plasma factors, for its delivery to the liver and adrenals for bile acid and steroid hormone synthesis, respectively. Arguably, the most prominent obstacle to a molecular understanding of these events is the lack of information on how the structure of apoA-I modulates HDL function. Most of our knowledge of apoA-I conformation was generated within the first few years of the publication of its primary structure (2), largely from theoretical analysis of the amphipathic α-helical repeats in the sequence (3, 4). Circular dichroism and infrared spectroscopy (IR) have shed light on the rough secondary structural contents of various forms of apoA-I (5, 6), but hard experimental evidence concerning the three-dimensional arrangement of these elements in the native protein is lacking.

Recently, an x-ray crystal structure of a lipid-free fragment of apoA-I was reported (7). The structure was a homotetramer of highly α-helical apoA-I molecules arranged in a ring with the monomers associating via the hydrophobic faces of their amphipathic α-helices. While the applicability of this structure to the native lipid-free forms of apoA-I is undetermined, this advance has rekindled an old debate on the structure of nascent, discoidal HDL particles. It is widely accepted that discoidal HDL particles reconstituted *in vitro* (rHDL) are composed of a patch of phospholipid/cholesterol bilayer stabilized at its edges by the amphipathic α-helices of apoA-I. Segrest *et al.* and others (8, 9) proposed early on that the α-helices were arranged around the circumference of the disc with the long axis of the helices perpendicular to the phospholipid (PL) acyl chains. This became known as the "belt" or "bicycle wheel" model. However, other investigators theorized that the 22 aa helical repeats were an ideal length to traverse the bilayer edge with the helices parallel to the acyl chains (10). This "picket fence" model has been favored in recent years because of supporting IR spectroscopy studies (6, 11) and the model's superb ability to account for the experimentally observed size classes of apoA-I containing rHDL (12). Borhani *et al.* (7) proposed that the ring shaped structure observed in their crystal was new evidence that the belt model may be correct. This view has been supported in recent months by methodologically updated IR experiments (13). A detailed computer analysis of the belt model has also been recently published (14).

To provide information on the three-dimensional structure of apoA-I, we have taken the approach of combining fluorescence spectroscopy with single Trp mutants of human proapoA-I. Our initial studies focused on lipid-free apoA-I (15). However, in light of the picket fence *versus* belt model debate and the conflicting IR data, our current study utilized a simple strategy to distinguish between the two models in discoidal rHDL par-

* This work was supported by a Grant RO1 HL62542 from the National Heart, Lung, and Blood Institute, National Institutes of Health (to W. S. D.). The costs of publication of this article were defrayed in part by the payment of page charges. This article must therefore be hereby marked "*advertisement*" in accordance with 18 U.S.C. Section 1734 solely to indicate this fact.

‡ To whom correspondence should be addressed: Dept. of Pathology and Laboratory Medicine, University of Cincinnati, 231 Bethesda Ave., Cincinnati, OH 45267-0529. Tel.: 513-558-3707; Fax: 513-558-2289; E-mail: sean.davidson@UC.edu.

[1] The abbreviations used are: apoA-I, apolipoprotein A-I; aa, amino acid residue; HDL, high density lipoprotein; rHDL, reconstituted HDL; PL, phospholipid; POPC, 1-palmitoyl,2-oleoyl phosphatidylcholine; STB, standard Tris buffer; W@108, a single Trp mutant containing Trp at position 108 with all other sites normally containing Trp converted to Phe; W@115, same as for W@108 except the Trp is at position 115; WT, wild type; DOXYL, another name for nitroxide spin label; NBD, nitrobenzoxadiazole; PSPC, 1-palmitoyl-2-steroyl phosphatidylcholine; SUV, small unilamellar vesicles.

ticles. We employed lipid-based quenching studies using rHDL reconstituted with the single Trp mutants and synthetic phospholipids containing nitroxide spin labels at various positions down the length of the fatty acyl chain. These labels can quench Trp residues in lipid interacting areas of proteins and are used in conjunction with a technique called the parallax analysis. This method has been used to accurately measure the depth of Trp penetration in transmembrane proteins (16–19). We have extended this analysis to the situation of apoA-I wrapping around a patch of lipid bilayer in rHDL particles. Our hypothesis was straight forward. If the picket fence model is correct, Trp residues at the center of a helical domain should be measured near the center of the bilayer in rHDL particles, whereas those near the ends of the domain should be considerably more shallow (see Figs. 1 and 2). If the belt model is correct, Trp residues should be measured at similar bilayer depths regardless of their location on the helix.

The results of this study suggest that at least helix 4 of apoA-I exists in the belt conformation in rHDL of various sizes. We believe this study provides one of the first measurements of the location of an apoA-I helix with respect to the bilayer edge.

EXPERIMENTAL PROCEDURES

Materials

1-Palmitoyl,2-oleoyl phosphatidylcholine (POPC), the nitroxide spin probes 1-palmitoyl,2-stearoyl(*X*-DOXYL)-*sn*-glycero-3-phosphocholine (where $X = 5$, 7, 10, 12, and 16), and 1-oleoyl,2-(12-NBD)-*sn*-glycero-3-phosphocholine were purchased from Avanti Polar Lipids (Birmingham, AL). The atomic phosphorus standard was obtained from Sigma. The single Trp synthetic peptides $K_2WL_9AL_9K_2A$ and $K_2GL_9WL_9K_2A$ were the generous gift of Dr. Erwin London at the State University of New York at Stony Brook. bis(sulfosuccinimidyl)suberate (BS_3) was purchased from Pierce. All other reagents were analytical grade.

METHODS

Mutagenesis, Protein Expression, and Purification—Human proapoA-I (containing the 6-aa prosegment) was used in this study because of its high expression level in bacteria and the lack of structural or functional differences from mature plasma apoA-I (20). To generate single Trp mutants, each of the five naturally occurring Trp residues (positions −3, 8, 50, 72, and 108) in proapoA-I were converted to Phe. This yielded a mutant that contained no Trp residues (W@ϕ). W@ϕ was then used as a template to re-insert a Trp residue at position 108 (W@108) and, in a separate mutant, to convert Tyr-115 to a Trp (W@115). The site-directed mutagenesis was accomplished using either standard polymerase chain reaction-based techniques or the QuickChange™ mutagenesis kit (Stratagene). The sequence of each construct was verified on an Applied Biotechnology System DNA sequencer. The resulting constructs were ligated into the PET-30 vector (Novagen) directly downstream of a histidine tag (His tag) sequence and transfected into BL-21 (DE3) *Escherichia coli* cells. The overexpression of the mutant proapoA-I was performed using freshly transfected cells as described previously (15). After harvesting, the cells were resuspended in 10 mM Tris buffer, pH 8.0, containing 0.15 M NaCl (standard Tris buffer, STB). The cells were lysed for 1 h at room temperature using B-PER lysis detergent (Pierce) at 4 ml of detergent solution for every 100 ml of bacterial cell culture. The soluble cell contents were applied to a His bind column (Novagen) and eluted according to manufacturer's instructions. The His-tagged proteins were dialyzed into 10 mM ammonium bicarbonate buffer, pH 8.0, and lyophilized. Lyophilized proteins were solubilized in 3 M guanidine HCl, dialyzed into STB to make rHDL particles (see below). The His tag was then removed by cleavage with 0.5 unit of enterokinase per 250 μg of proapoA-I at 25 °C for 16 h. The intact proapoA-I containing rHDL particles were purified away from the enterokinase and the cleaved His tag by gel filtration chromatography on a Superdex 200 (Amersham Pharmacia Biotech) column. Proteins prepared by this method were >95% pure as visualized by SDS electrophoresis stained with Coomassie Blue and the yields were about 5 mg of protein/100 ml of original culture.

Preparation and Characterization of the Lipid-containing Particles—rHDL particles were prepared as described previously (21) using POPC, mutant proapoA-I and spin-labeled phospholipids. All phospholipid stock solutions were assayed before the reconstitution by the phosphorus method of Sokoloff and Rothblat (22). Initial lipid to protein molar ratios were 85:15:1 (POPC:DOXYL-PSPC:proapoA-I) to isolate the 98- and 160-Å particles and 34:6:1 (POPC:DOXYL-PSPC:proapoA-I) to isolate the 78- and 90-Å particles. For each mutant, a set of particles was reconstituted without the spin-labeled phospholipids. The different particle sizes were isolated by gel filtration chromatography on a Superdex 200 gel filtration column (23) to remove any unreacted protein and vesicular structures. To ensure that the gel filtration step did not change the concentration of quencher within the particles, we performed control experiments using rHDL preparations that contained 12-NBD-PC. The various DOXYL quenchers were able to quench this label identically whether in complexes studied prior to or after gel filtration chromatography. The phosphorus assay and the Markwell modification of the Lowry protein assay (24) determined the final lipid and protein concentrations. Particle hydrodynamic diameters were measured by gradient native polyacrylamide electrophoresis (23). The number of apolipoprotein molecules per rHDL complex was determined by BS_3 cross-linking (25). The secondary structure content of the proapoA-I in the rHDL particles was estimated by circular dichroism at 222 nm (23).

Small unilamellar vesicles (SUV) containing the transmembrane peptides were prepared as by Ren *et al.* (26). For all peptide experiments, the lipid to protein molar ratios were 68:12:1 (POPC:DOXYL-DSPC:peptide). The appropriate lipids in chloroform were dried under nitrogen for at least 2 h. The appropriate amount of peptide was applied to the lipids in a volume of 10 μl absolute ethanol. The lipid/peptide mixture was vortexed, incubated on ice for 10 min, and then diluted to 1 ml with filtered STB. The small amount of ethanol in the mixture has been shown not to interfere with the fluorescence characteristics of the sample (18). The final concentrations of lipid in the samples were 200 μM. Identical samples were made containing POPC SUV only (blank for fluorescence runs) and POPC SUV with peptide in the absence of spin label (for determination of F_o).

Fluorescence Spectroscopy—All fluorescence measurements were performed on a Photon Technology International Quantamaster spectrometer in photon counting mode. The emission and excitation band passes were 3.0 nm. The excitation wavelength for all Trp studies was 295 nm to minimize the contribution of tyrosine fluorescence in proapoA-I. The samples (in STB for all studies) were measured at 25 °C in a semimicro quartz cuvette. The emission spectra from 303 to 375 nm were corrected for the background fluorescence of either buffer alone (rHDL samples) or SUV alone in buffer (peptide samples). The spectra were not corrected for the spectral characteristics of the emission and excitation monochromators.

Depth Calculations, Theory—The parallax method for determining the depth of penetration of a fluorophore into a lipid bilayer was derived by Chattopadhyay and London (27) from classical relationships of static quenchers to randomly distributed fluorophores. The method depends on the differences in fluorescence intensities of the fluorophore in the presence of known concentrations of nitroxide quencher groups at known locations in a phospholipid acyl chain. Since quenching is a distance-dependent phenomena, the quenching ratio from two quenchers, one shallow and one deep in the membrane, are used calculate the relative depth of the fluorophore relative to the quenchers. The method was initially applied to lipid-based fluorescent groups that are exposed to quencher on all sides and both leaflets of the bilayer. The theory was later modified to allow for the quenching of Trp residues on transmembrane peptides (18). The distance of the Trp from the center of the bilayer (Z_{cf}) is given by,

$$Z_{cf} = L_{cs} + [-\ln(F_s/F_d)/\pi C - L_{ds}^2]/2L_{ds} \quad \text{(Eq. 1)}$$

where F_s is the fluorescence intensity in the presence of the shallow quencher, F_d is the same for the deep quencher, L_{cs} is the distance from the center of the bilayer to the shallow quencher, L_{ds} is the distance between the shallow and deep quenchers, and C is the concentration of the quencher molecules per Å^2. Equation 1 holds when the Trp residue is quenched by nitroxide groups in the same leaflet of the membrane as the Trp. However, in the case where the Trp is deeply buried within the membrane, it is subjected to quenching from groups in the opposing leaflet of the membrane as well. For this situation, a second relationship is required to account for trans-bilayer quenching,

$$Z_{cf} = L_{cd} - [\ln((F_S/F_o)^2/(F_d/F_o))/\pi C) - 2L_{ds}^2 + 4L_{cd}^2)/4(L_{ds} + L_{cd})] \quad \text{(Eq. 2)}$$

where F_o is the fluorescence intensity in the absence of quencher, L_{cd} is the distance from the center of the bilayer to the deep quencher, and L_{ds} is the distance between the shallow and deep quenchers. For a detailed discussion and the derivation of these equations, see Refs. 18 and 33. Equation 2 was used in this study whenever a Trp residue was deter-

mined to be <5 Å from the center of the membrane by Equation 1. These equations have been demonstrated to accurately describe the behavior of single Trp transmembrane helices in model membrane systems (18).

Although, in theory, any pair of quenchers can be used for the analysis, the quenching pair of C-5 and C-12 was chosen for our calculations for two important reasons. First, in the case of our rHDL particles, these two quenchers gave the largest difference in quenching efficiencies (Fig. 3). Where the data was available, we also calculated depth using the C-5/C-10 and the C-5/C-7 quencher pairs. While these gave similar mean values, the standard deviations among the values between samples were consistently 2–3-fold higher than with the C-5/C-12 quencher pairs. Second, Abrams and London (17) have published detailed information on the quenching of 12-NBD phospholipids using the C-5/C-12 pair. The NBD quenching data allowed the calibration of our particular batches of spin-labeled lipid to estimate Trp depths as accurately as possible (see below). For the quenchers at positions 5 and 12, the relevant depth values were: L_{cs} = 12.15 Å, L_{ds} = 6.3 Å, and L_{cd} = 5.85 Å.

The *C* term is the mole fraction of spin-labeled lipids divided by the average area occupied by a lipid molecule, 70 Å^2 (17). For a fluorophore that is surrounded on all sides by quencher (as is the case for the transmembrane peptides used in this study), *C* was calculated using the mole fraction value of 0.15 (the fraction of label for all particles in this study). However, in the case of the rHDL particle, the Trp residue is on the edge of the bilayer and is only exposed to the lipid on one side. Since the diameter of a phospholipid molecule is small compared with the diameter of the rHDL disc, the Trp in a rHDL particle is expected to have a lipid exposure that is about 50% that of a free floating peptide. Thus, a mole fraction of 0.075 was used to calculate *C* for all of the rHDL particles in this study.

Spin Label Assay—The spin label content of the purchased spin-labeled phospholipids was measured as suggested by Abrams and London (17). These authors have reported F/F_o values for the quenching of 12-NBD-PC in PBS at pH 7 in SUV in the presence of the DOXYL-5 and DOXYL-12 phospholipids present at 10 mol %. The spin label/phosphorus ratio for the particular batch of spin labels had been previously calibrated against known standards by electron spin resonance (ESR) spectroscopy. As an ESR machine was not available for calibration in our work, we performed the same quenching experiments. We determined that our batch of lipids contained an average of 0.95 spin labels/mol of phosphorus. This factor was taken into account during the reconstitutions of the rHDL and SUV used in this study.

RESULTS

Experimental Design—To determine the orientation of apoA-I helices with respect to the lipid bilayer, we produced two single Trp mutants of proapoA-I, one containing a Trp at position 108 and the other containing a Trp at position 115. Both of these sites occur in the putative helical repeat 4 (as numbered by Roberts *et al.* (28)). This region was chosen because (*a*) it already contained a naturally occurring Trp at position 108 and (*b*) repeat 4 is punctuated on both ends with a Pro residue and is universally predicted to exist entirely as a α-helix in rHDL particles (29–31). Both Trp residues at pos. 108 and 115 are predicted to be in the center of the hydrophobic face of the helix as one looks down the long axis of the repeat (Fig. 1) and likely interact with lipid. However, when one looks perpendicular to the long axis of the helix (from a side view, as in Fig. 2), Trp-108 is near the center of the helix, roughly equidistant from the N- and C-terminal Pro residues that punctuate the repeat. Trp-115, however, is two helical turns C-terminal to Trp-108, about 12 Å closer to Pro-121. The hypothesized predictions for lipid quenching studies using these two mutants in nitroxide label-containing rHDL are shown in Fig. 2. If the helix is in the picket fence orientation, Trp-108 should be situated near the center of the membrane and Trp-115 should be substantially more shallow. If the helix is in the belt orientation, both Trp residues should exhibit similar depths and will be situated some distance up each leaflet in the bilayer.

In our initial experiments, each of the two single Trp mutants were reconstituted with phospholipids containing quenchers at each of the five commercially available positions

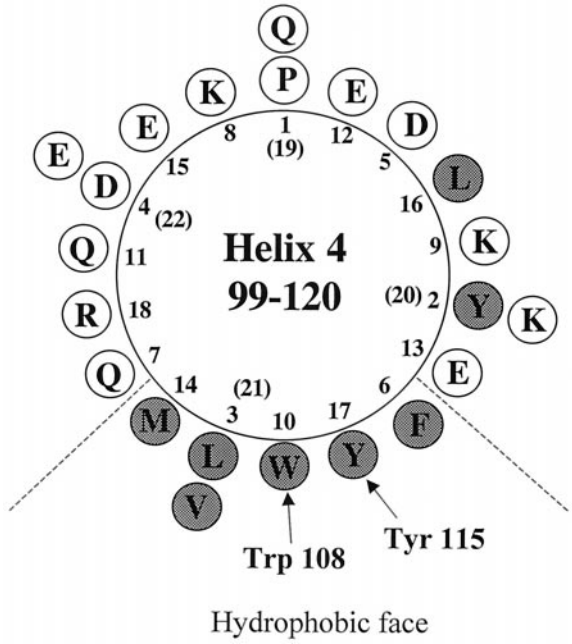

FIG. 1. **Helical wheel diagram of helix 4 in human apoA-I.** The diagram shows the distribution of the amino acids from 99 to 120 in apoA-I, with Pro-99 being represented as position 1 in the helix. Hydrophilic and neutral amino acids are in *white* and hydrophobic amino acids are in *gray*. Notice that Trp-108 is shown to be in the center of the hydrophobic face of the helix. Tyr-115, which was converted to a Trp in this study, is two α-helical turns C-terminal to Trp-108 (3.6 aa per turn) and is also near the center of the hydrophobic face.

along the phospholipid acyl chain (C-5, -7, -10, -12, and -16). A sixth preparation contained POPC only. The first set of reconstitutions was performed at 100:1 (mole of PL:mole of proapoA-I). The reaction mixture produced two populations of rHDL particles of 160 and 98 Å in diameter that were easily separated by gel filtration. To obtain information about particles that contained only two molecules of proapoA-I per particle, a second set of reconstitutions was performed at a PL:proapoA-I molar ratio of 40:1. In this series, the particles were only made with quenchers at positions C-5 and C-12 for the parallax analysis (for cost reasons) resulting in two populations of 93 and 76Å in diameter. These were also isolated by gel filtration.

Characterization of the Various Size rHDL—The use of the Trp mutants in fluorescence studies depends on the assumption that the amino acid replacements do not perturb the structure and function of the WT proapoA-I. In previous work, we have characterized W@108 in detail and determined that it was similar to WT using several indices of protein structure and function (15). Table I lists the physical characteristics of the four particle size classes made with W@108 and W@115 in this study. Both mutants formed rHDL particles of similar size classes as measured by native polyacrylamide gradient gel electrophoresis. A comparison between the two mutants within a given size class indicates that they were of similar phospholipid to protein molar composition and similar numbers of proapoA-I molecules per particle. Also, within each size class, their fractional α-helical contents were similar as measured by far UV circular dichroism. These data are consistent with previous studies in which rHDL particles of these sizes were generated with human plasma apoA-I (23, 25), indicating that the mutations in both mutants do not affect the structure and composition of the rHDL particles. It was also important to verify that the presence of the nitroxide spin labels did not adversely affect the rHDL particles. Each value in Table I is an average of data taken from complexes containing POPC only, 5-DOXYL and 12-DOXYL (and 7-, 10-, and 16- in the case of the

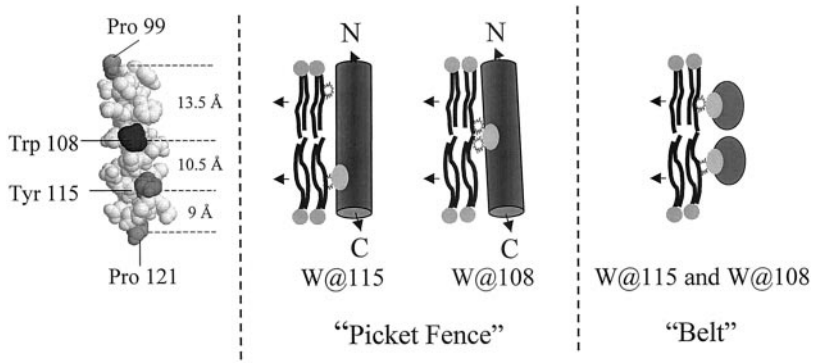

FIG. 2. **Predictions of Trp location with respect to the bilayer for the picket fence and belt models.** *Left side*, the x-ray structure of helix 4 of apoA-I from Borhani *et al.* (7) showing the punctuating Pro residues and the positions of amino acids 108 and 115 along the helix. *Center*, the interaction of helix 4 at the edge of a phospholipid bilayer is depicted as a cross-section through a rHDL particle (a side view). Quenching groups on the acyl chains of the phospholipids are represented by the *star symbols*. The *cylinders* represent helix 4 in apoA-I. The *light circles* indicate Trp residues. The nomenclature W@X indicates a mutant in which a Trp residue exists at position *X* only, and all other sites that normally contain Trp have been converted to Phe. *Picket fence* prediction: if helix 4 of apoA-I exists in this orientation, then quenching groups placed at the center of the membrane (closer to carbon 16) should maximally quench W@108 in rHDL particles whereas quenching groups near carbon 5 should exhibit reduced quenching. W@115, on the other hand, should be maximally quenched nearer the surface of the bilayer and less so near the center. *Right side*, *Belt* prediction: in this case, both Trp residues should be quenched at similar depths in the membrane. Furthermore, they should be situated some distance away from the center of the bilayer (*i.e.* some distance up each leaflet).

TABLE I
Characterization of the various sized reconstituted HDL particles

Protein component[a]	Diameter (±3 Å)[b]	PL:proapoA-I	No. proapoA-I/ particle[c]	α-Helix content[d]	λ_{max} (±2 nm)
		mol:mol		%	
W@108	162	135 (±7):1	>4	75 (±4)	330
	98	90 (±6):1	3	72 (±2)	327
	93	80 (±4):1	2	87 (±4)	324
	78	55 (±6):1	2	57 (±3)	330
W@115	160	135 (±11):1	>4	81 (±4)	332
	98	91 (±3):1	3	76 (±2)	328
	90	85 (±6):1	2	86 (±4)	333
	77	63 (±9):1	2	53 (±4)	334

[a] All data presented in this table are average values for each size class of particles derived from all particles regardless of DOXYL content. For example, the PL:proapoA-I ratio data derived for the W@108 162-Å particle was averaged from the particles containing no spin label, DOXYL-5, -7, -10, -12, and -16.

[b] The Stokes diameter as determined by native polyacrylamide gel electrophoresis. The error of 0.3 nm is based on maximal S.D. values obtained for multiple determinations of similarly sized particles in previous studies (23). All complexes were judged to be >95% pure by coomassie densitometry with the exception of the 77–78-Å particles which had about 10–15% contamination with the 90–93-Å particle.

[c] The α-helical contents were determined from the molar ellipticity at 222 nm at 25 °C as calculated according to (38). Each value represents the average of at least three observations.

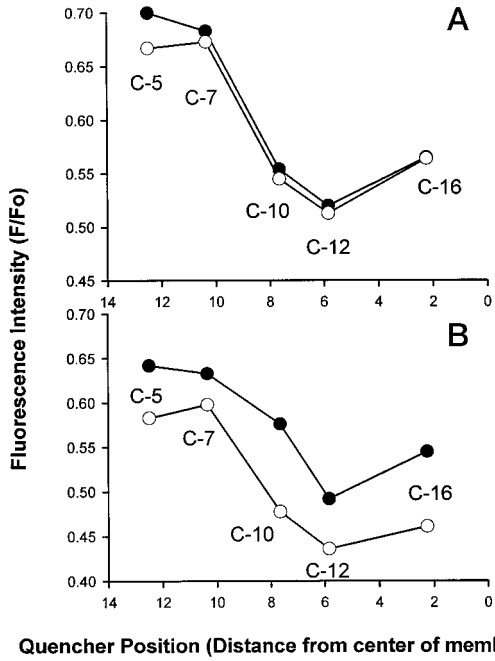

FIG. 3. **Nitroxide lipid quenching of proapoA-I single Trp mutants in 98 (*A*) and 160-Å rHDL particles (*B*).** The rHDL particles were prepared with each mutant at a molar ratio of 85:15:1 mol:mol (POPC:DOXYL-X PSPC:proapoA-I). The 98- and 160-Å size classes were separated by gel filtration chromatography, characterized, and used for fluorescence studies at concentrations of 75 μg of proapoA-I/ml in STB. The emission spectra were collected from 303–375 nm and the fluorescence intensity (*F*) for the DOXYL containing samples at the λ_{max} was plotted as a ratio of the fluorescence of the same particle without quenching groups present (F_o). The excitation wavelength was 295 nm. The labels near each data point indicate the carbon number of the phospholipid acyl chain that contained the quenching group. The *x* axis shows the distance of each DOXYL group from the center of the membrane (C-5, 12.15 Å; C-7, 10.35 Å, C-10, 7.65 Å; C-12, 5.85 Å, and C-16, 2.25 Å). In both panels: *open circles*, W@108; *filled circles*, W@115.

98- and 160-Å particles) for a given mutant in a given size class. A student's *t* test performed within each set of data failed to identify a significant structural or compositional difference among the particles with or without the DOXYL quenchers, regardless of position. Table I also lists the wavelength of maximum fluorescence (λ_{max}) measured for each complex. All rHDL particles exhibited blue-shifted λ-max values, which are consistent with the Trp residues being involved in lipid contacts (32). We also determined that W@108 and W@115 in rHDL particles were not significantly quenched by the soluble quencher acrylamide (data not shown). This indicates that the Trp residues were not exposed to the aqueous buffer and, therefore, were appropriate for lipid-based quenching studies.

Fluorescence Quenching of the Lipid-bound Proteins—Once the particles were characterized, the fluorescence intensity of the Trp residue in the absence of quencher was compared with those in the presence of the nitroxide-labeled phospholipids. The results are shown in Fig. 3. In the case of the 98-Å particles (Fig. 3*A*), the shallowest quencher at carbon 5 (C-5) in the acyl chain minimally quenched the fluorescence of Trp-108. As the quencher depth was increased, Trp-108 fluorescence was increasingly quenched to a maximum near C-12 and then decreased at C-16. The Trp at position 115 followed a nearly identical pattern. The data were remarkably consistent between experiments; similar results were obtained in three experiments performed on three independently prepared sets of

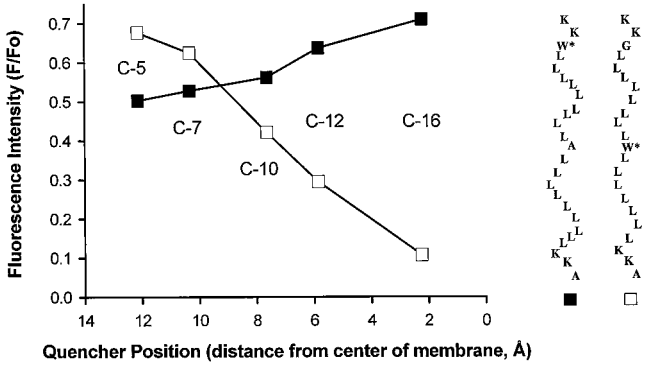

FIG. 4. **Nitroxide lipid quenching of single Trp-containing, transmembrane peptides in SUV.** The SUV containing each peptide was prepared by ethanol dilution as described under "Methods" at a molar ratio of 68:12:1 (POPC:*X*-DOXYL PSPC:peptide). The samples were used for fluorescence studies under the same conditions described for Fig. 3, and the data were plotted the same way. The peptide $K_2WL_9AL_9K_2A$ data are shown with the *filled squares* and that for $K_2GL_9WL_9K_2A$ is shown with the *open squares*. The schematic illustrations to the *right* of the figure show the sequence of each peptide, highlighting the location of the Trp residue in each.

rHDL particles. Analogous quenching patterns were found using the largest 160-Å particles containing the same array of quenchers (Fig. 3*B*).

We performed a positive control experiment to convince ourselves that the quenching protocol was capable of determining the orientation of helices that are known to be parallel to the acyl chains in a bilayer. We used two hydrophobic α-helical peptides that each contained a single Trp residue at different points along the length of the helix (gifts of Dr. Erwin London). Ren *et al.* (18) have demonstrated that these synthetic peptides traverse the membrane of SUV and are, necessarily, oriented parallel to the acyl chains. Peptide $K_2WL_9AL_9K_2A$ contains a 22-aa transmembrane domain composed largely of repeating leucines flanked with pairs of lysine residues (Fig. 4). The lysines stabilize the ends of the helix in the polar region of the bilayer and allow the intervening hydrophobic region to stretch across the acyl chains. The Trp in this peptide is situated high in the membrane, just below the lysine residues. Peptide $K_2GL_9WL_9K_2A$ is similar in design, but the Trp has been moved halfway down the length of the hydrophobic region of the helix. We reconstituted these peptides into SUV and performed lipid-quenching studies similar to those performed with the rHDL particles (Fig. 4). As expected, the Trp in $K_2WL_9AL_9K_2A$ was maximally quenched when the quencher was at C-5. The quenching decreased as the spin label was moved down the acyl chains. $K_2GL_9WL_9K_2A$ exhibited the opposite quenching pattern; the deeply situated Trp was minimally quenched near the surface of the bilayer and was maximally quenched near C-16, close to the bilayer center.

To quantitate the location of the Trp residues with respect to the bilayer, the distance of each Trp from the center of the bilayer (Z_{cf}) was calculated using the parallax analysis (27). Table II lists the data for each of the rHDL size classes. In the case of rHDL particles containing Trp-108, the Trp depth was found to range from 5.6 to 6.6 Å with an average of 6.2 Å for all four size classes. The Trp depth was not statistically different from the average for any size class. Similar results were obtained for the W@115 particles, which ranged from 5.0 to 6.0 Å with an average of 5.5 Å. It appears that our extension of the parallax method to the case of an rHDL particle is satisfactory because the calculated Trp depths in Table II agree well with qualitative judgments that one would make as to the depth of the most effective quencher in Fig. 3. Therefore, these data indicate that the Trp residues at positions 108 and 115 were

TABLE II
Determinations of Trp location with respect to the bilayer using mutant proapoA-I in rHDL particles

Protein (rHDL size)	F/F_o[a]		Zcf[b]
	5-DOXYL	12-DOXYL	
			Å
W@108 (162 Å)	0.54 (±0.04)	0.40 (±0.03)	6.5 (±0.6)
W@108 (98 Å)	0.69 (±0.09)	0.56 (±0.08)	5.9 (±0.7)
W@108 (93 Å)	0.61 (±0.12)	0.51 (±0.02)	6.6 (±0.3)
W@108 (78 Å)	0.67 (±0.05)	0.52 (±0.02)	5.6 (±0.1)
			Average: 6.2 (±0.5)
W@115 (160 Å)	0.64 (±0.04)	0.48 (±0.02)	5.6 (±0.2)
W@115 (98 Å)	0.61 (±0.13)	0.45 (±0.09)	6.0 (±0.9)
W@115 (90 Å)	0.72 (±0.02)	0.58 (±0.02)	5.4 (±0.1)
W@115 (77 Å)	0.80 (±0.02)	0.67 (±0.02)	5.0 (±0.2)
			Average: 5.5 (±0.4)

[a] The term F is the fluorescence intensity in the presence of the indicated DOXYL group. F_o is the intensity in the absence of quencher.
[b] The calculated distance from the center of the bilayer to the single Trp residue in each molecule of proapoA-I in the various size rHDL determined from Equation 2 (see "Methods"). The S.D. are calculated from at least three observations.

TABLE III
Determinations of Trp location with respect to the bilayer in control transmembrane peptides in small unilamellar vesicles

Peptide	F/F_o		Zcf[a]	λ_{max} (±2 nm)
	DOXYL-5	DOXYL-12		
			Å	
$K_2GL_9WL_9K_2A$	0.58 (±0.1)	0.22 (±0.1)	3.1 (±0.6)	317
$K_2WL_0AL_9K_2A$	0.35 (±0.2)	0.51 (±0.1)	14.0 (±3.0)	333

[a] The calculated distance from the center of the bilayer to the single Trp residue per molecule of peptide from Equation 1 or 2 (see "Methods"). The S.D. are calculated from at least three observations.

located at similar depths in the membrane and this did not vary significantly with the size or number of proapoA-I molecules in the rHDL particle. In the case of the control peptides (Table III), the average distance of the Trp residue from the bilayer center for $K_2WL_9AL_9K_2A$ was determined to be about 14 Å, while that for $K_2GL_9WL_9K_2A$ was about 3 Å. These values compare favorably with the previously published values (18) for these peptides. The λ_{max} values for the peptides were increasingly blue shifted with the depth of penetration of the Trp residue into the membrane (18).

DISCUSSION

Lipid-based quenching experiments and the parallax analysis have been useful for defining the positions of Trp residues in transmembrane proteins (33). Here, we have extended this method to the related situation of apoA-I wrapping around the outside of a phospholipid bilayer (see "Methods") to determine the orientation of helix 4 with respect to the bilayer. Our results are discussed below in terms of the picket fence and belt models introduced in Fig. 2.

If one assumes that helix 4 is in the picket fence orientation, Trp-108 should be situated about 3 Å from the center of the membrane (assuming that the geometric center of the helix (99–121) is residue 110 and a 1.5-Å rise per α-helical residue). Trp-115 should then be about 8 Å from the bilayer center on the opposing leaflet. However, Table II shows that both Trp residues were consistently measured at similar depths of about 6 Å in the various particles. In contrast, the Trp residue in peptide $K_2WL_9AL_9K_2A$ was measured at 14 Å from the center of the bilayer, in excellent agreement with the picket fence theoretical value of 13.5 Å. The Trp residue in peptide $K_2GL_9WL_9K_2A$ was measured at 3 Å from the center, reasonably close to the theoretical value of 1.5 Å. Thus, the data for the transmembrane peptides are most consistent with the picket fence model

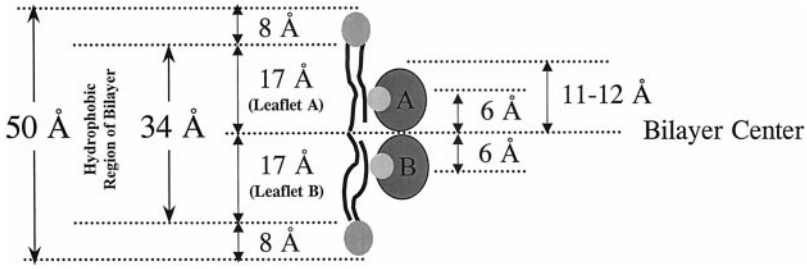

FIG. 5. **A model for the orientation and localization of helices in rHDL particles.**

prediction (as expected), whereas the data for helix 4 of apoA-I are most consistent with the prediction for the belt model. It may be argued, however, that the data for helix 4 can be consistent with the picket fence model if the helix were moved 3–4 Å across the bilayer in the direction of the N terminus. This would have the effect of pulling Trp-108 away from the bilayer center and Trp-115 toward the center. While our current data cannot preclude this possibility, we believe that this scenario is less likely because such an arrangement would require turn sequences that are no longer centered on Pro residues. The helix breaking propensity of Pro has been proposed to be an important requirement for the rather sharp helical turns required by the picket fence model.

If we assume that helix 4 is in a belt orientation, it is possible to construct the model in Fig. 5. We assumed that the total bilayer width for a liquid crystalline POPC bilayer is 50 Å as measured by x-ray reflection techniques (15 mol % H_2O at 23 °C) (34). Of that, 8 Å is attributed to the polar head group regions of each leaflet (16 Å total), leaving 34 Å for the hydrophobic portion of the membrane. This gives two leaflets of about 17 Å that must be in contact with apoA-I to prevent unfavorable solvation of the acyl chains. We further assumed that one helix interacts with each leaflet as proposed for the belt model (7, 14), although we make no suggestion of the identity of the second helix. Our quenching measurements placed the Trp residues of helix 4 of apoA-I about 5.5–6 Å from the center of the bilayer (Table II). Since the Trp residues were located near the centerline of the hydrophobic region of the helix (Fig. 1), this predicts that there were about 12 Å between the centers of the two helices. Our analysis of the x-ray crystal structure for the lipid-free variant of apoA-I (7) indicates that there is an average of 10–11 Å between centers of helix 4 and helix 6 of a second apoA-I molecule in the structure. Therefore, assuming a typical apoA-I helical radius of about 5.5 Å, our fluorescence measurements are consistent with the edges of the α-helices in rHDL particles being clustered together at the center of the bilayer. Furthermore, they appear to be close enough to each other for possible salt bridge interactions such as those proposed for the belt model (14).

It is interesting to note that if the analysis of the helical radii and the placement of the helices by the fluorescence measurements are correct, then two helices together can only account for 22–24 Å of the total 34 Å of acyl chain region. The reasons for this apparent shortfall are not entirely clear although physical measurements on rHDL particles made in the past have suggested that protein to phospholipid interactions at the disc edge can account for a reduced bilayer thickness at the perimeter *versus* that in the center of the particle (35). It is also possible that the phospholipid head groups can bend slightly around the sides of the helices to interact with negative charges along the polar surface of the helix, shortening the effective distance that the protein needs to cover. Such phospholipid to amphipathic helix interactions have been proposed to occur on the surface of spherical HDL particles or vesicles (36, 37).

Another informative observation in this work was that the Trp depths were similar in rHDL that contained 2, 3, and >4 molecules of apoA-I per particle. Segrest *et al.* (14) have suggested that when two apoA-I molecules are present in a complex, they are arranged on top of each other in a staggered, anti-parallel fashion with each C-shaped molecule wrapping entirely around a leaflet of the bilayer. In this model, the helix A depicted in the cross-section in Fig. 5 would come from one molecule of apoA-I, while helix B would come from the other. Four molecules of apoA-I can be envisioned in this scenario by simply opening up the original two molecules and slipping in two more to surround a larger lipid patch (7, 14). However, three molecules of apoA-I are more difficult to envision because the two leaflets are already occupied. Therefore, if the helices are perpendicular to the acyl chains and to fit three molecules on two leaflets, one is forced into postulating that the molecules of apoA-I can double back on themselves. In this scenario, half of each molecule is on leaflet A, there is an intervening turn, and the other half of the molecule proceeds back toward the N terminus on leaflet B. In this model, helices A and B in Fig. 5 would be from the same molecule of apoA-I. This allows the presence of both even and odd numbers of apoA-I on a particle. Our experimental approach in this study was incapable of distinguishing between these two variants of the belt model, but we feel that this "double back" belt model is the simplest explanation for our observation of three molecules of apoA-I in a rHDL particle with helices consistent with the belt configuration.

Finally, it is important to note that these results apply only to helix 4, and they do not exclude the possibility that some areas of apoA-I may exist in a belt conformation, while others exist in a picket fence or other orientation. More Trp residues will have to be introduced in other helical areas of the molecule to investigate this possibility. We believe that the strategy of using carefully designed single Trp mutants with lipid-based quenching studies is a promising approach for understanding the structure of apoA-I and HDL. In addition, we are excited about the potential of this method for structural studies of other apolipoproteins, in both discoidal and spherical HDL particles.

Acknowledgments—We are indebted to Dr. Erwin R. London (State University of New York at Stony Brook) for providing the transmembrane peptides, calibration data, and valuable advice and discussion concerning the use of the parallax analysis.

REFERENCES

1. Scanu, A. M., and Wisdom, C. (1972) *Annu. Rev. Biochem.* **41,** 703–730
2. Baker, H. N., Gotto, A. M. J., and Jackson, R. L. (1975) *J. Biol. Chem.* **250,** 2725–2738
3. McLachlan, A. D. (1977) *Nature* **267,** 465–466
4. Segrest, J. P., Jackson, R. L., Morrisett, J. D., and Gotto, A. M. J. (1974) *FEBS Lett.* **38,** 247–258
5. Lux, S. E., Hirz, R., Shrager, R. I., and Gotto, A. M. (1972) *J. Biol. Chem.* **247,** 2598–2606
6. Wald, J. H., Coormaghtigh, E., De Meutter, J., Ruysschaert, J. M., and Jonas, A. (1990) *J. Biol. Chem.* **265,** 20044–20050
7. Borhani, D. W., Rogers, D. P., Engler, J. A., and Brouillette, C. G. (1997) *Proc. Natl. Acad. Sci. U. S. A.* **94,** 12291–12296
8. Segrest, J. P. (1977) *Chem. Phys. Lipids* **18,** 7–22
9. Wlodawer, A., Segrest, J. P., Chung, B. H., Chiovetti, R. J., and Weinstein,

J. N. (1979) *FEBS Lett.* **104,** 231–235
10. Tall, A. R., Small, D. M., Deckelbaum, R. J., and Shipley, G. G. (1977) *J. Biol. Chem.* **252,** 4701–4711
11. Brasseur, R., De Meutter, J., Vanloo, B., Goormaghtigh, E., Ruysschaert, J. M., and Rosseneu, M. (1990) *Biochim. Biophys. Acta* **1043,** 245–252
12. Wald, J. H., Krul, E. S., and Jonas, A. (1990) *J. Biol. Chem.* **265,** 20037–20043
13. Koppaka, V., Silvestro, L., Engler, J. A., Brouillette, C. G., and Axelsen, P. H. (1999) *J. Biol. Chem.* **274,** 14541–14544
14. Segrest, J. P., Jones, M. K., Klon, A. E., Sheldahl, C. J., Hellinger, M., De Loof, H., and Harvey, S. C. (1999) *J. Biol. Chem.* **274,** 31755–31758
15. Davidson, W. S., Arnvig-McQuire, K., Kennedy, A., Kosman, J., Hazlett, T., and Jonas, A. (1999) *Biochemistry* **38,** 14387–14395
16. Ghosh, A. K., Rukmini, R., and Chattopadhyay, A. (1997) *Biochemistry* **36,** 14291–14305
17. Abrams, F. S., and London, E. (1993) *Biochemistry* **32,** 10826–10831
18. Ren, J., Lew, S., Wang, Z., and London, E. (1997) *Biochemistry* **36,** 10213–10220
19. Chung, L. A., Lear, J. D., and DeGrado, W. F. (1992) *Biochemistry* **31,** 6608–6616
20. McGuire, K. A., Davidson, W. S., and Jonas, A. (1996) *J. Lipid. Res.* **37,** 1519–1528
21. Jonas, A. (1986) *Methods Enzymol.* **128,** 553–582
22. Sokoloff, L., and Rothblat, G. H. (1974) *Proc. Soc. Exp. Biol. Med.* **146,** 1166–1172
23. Davidson, W. S., Rodrigueza, W. V., Lund-Katz, S., Johnson, W. J., Rothblat, G. H., and Phillips, M. C. (1995) *J. Biol. Chem.* **270,** 17106–17113
24. Markwell, M. A., Haas, S. M., Bieber, L. L., and Tolbert, N. E. (1978) *Anal. Biochem.* **87,** 206–210
25. Jonas, A., Kezdy, K. E., and Wald, J. H. (1989) *J. Biol. Chem.* **264,** 4818–4824
26. Ren, J., Lew, S., Wang, J., and London, E. (1999) *Biochemistry* **38,** 5905–5912
27. Chattopadhyay, A., and London, E. (1987) *Biochemistry* **26,** 39–45
28. Roberts, L. M., Ray, M. J., Shih, T. W., Hayden, E., Reader, M. M., and Brouillette, C. G. (1997) *Biochemistry* **36,** 7615–7624
29. Nolte, R. T., and Atkinson, D. (1992) *Biophys. J.* **63,** 1221–1239
30. Calabresi, L., Meng, Q. H., Castro, G. R., and Marcel, Y. L. (1993) *Biochemistry* **32,** 6477–6484
31. Segrest, J. P., Jones, M. K., De Loof, H., Brouillette, C. G., Venkatachalapathi, Y. V., and Anantharamaiah, G. M. (1992) *J. Lipid. Res.* **33,** 141–166
32. Burstein, E. A., Vedenkina, N. S., and Ivkova, M. N. (1973) *Photochem. Photobiol.* **18,** 263–279
33. Ladokhin, A. S. (1999) *Biophys. J.* **76,** 946–955
34. Small, D. M. (1986) in *The Physical Chemistry of Lipids: From Alkanes to Phospholipids*, pp. 475–517, Plenum Press, New York
35. Andrews, A. L., Atkinson, D., Barratt, M. D., Finer, E. G., Hauser, H., Henry, R., Leslie, R. B., Owens, N. L., Phillips, M. C., and Robertson, R. N. (1976) *Eur. J. Biochem.* **64,** 549–563
36. Lecompte, M. F., Bras, A. C., Dousset, N., Portas, I., Salvayre, R., and Ayrault-Jarrier, M. (1998) *Biochemistry* **37,** 16165–16171
37. Mishra, V. K., Palgunachari, M. N., Segrest, J. P., and Anantharamaiah, G. M. (1994) *J. Biol. Chem.* **269,** 7185–7191
38. Chen, Y. H., Yang, J. T., and Martinez, H. M. (1972) *Biochemistry* **11,** 4120–4131